



Universidad Autónoma
de Madrid

Biblos-e Archivo
Repositorio Institucional UAM

Repositorio Institucional de la Universidad Autónoma de Madrid

<https://repositorio.uam.es>

Esta es la **versión de autor** del artículo publicado en:

This is an **author produced version** of a paper published in:

Phytochemistry 180 (2020): 112529

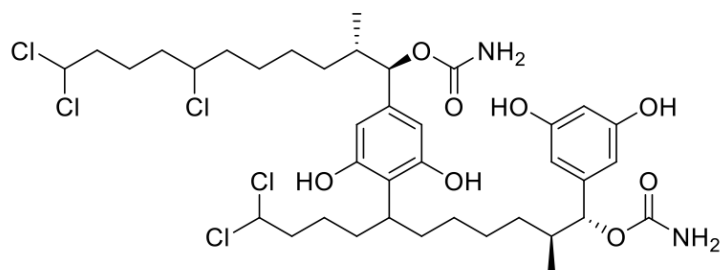
DOI: <https://doi.org/10.1016/j.phytochem.2020.112529>

Copyright: © 2020 Elsevier Ltd. This manuscript version is made available under the CC-BY-NC-ND 4.0 licence <http://creativecommons.org/licenses/by-nc-nd/4.0/>

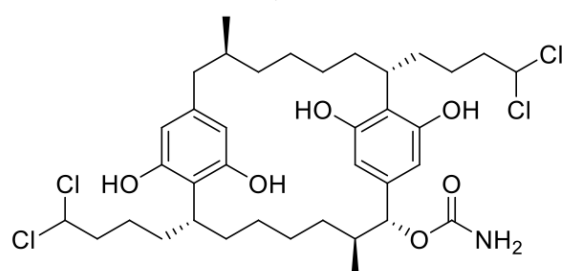
El acceso a la versión del editor puede requerir la suscripción del recurso

Access to the published version may require subscription

Antitumoral potential of carbamidocyclophanes and carbamidocylindrofridin A isolated from the cyanobacterium *Cylindrospermum stagnale* BEA 0605B



Carbamidocylindrofridin A



Carbamidocyclophane V



Antitumoral potential of carbamidocyclophanes and carbamidocylindrofridin A isolated from the cyanobacterium *Cylindrospermum stagnale* BEA 0605B

Víctor Tena Pérez^a, Luis Apaza Ticona^{a,b,*}, Alfredo H. Cabanillas^a, Santiago Maderuelo Corral^c, Josefina Perles^e, Diego Fernando Rosero Valencia^c, Antera Martel Quintana^d, Montserrat Ortega Domenech^{c,*}, Ángel Rumbero Sánchez^a

Affiliation

^a*Department of Organic Chemistry, Faculty of Sciences, University Autónoma of Madrid. Cantoblanco, 28049 Madrid, Spain*

^b*Department of Pharmacology, Pharmacognosy and Botany, Faculty of Pharmacy, University Complutense of Madrid. Ciudad Universitaria s/n, 28040 Madrid, Spain*

^c*Valoralia I más D SLU, Tres Cantos, 28760 Madrid, Spain.*

^d*Spanish Algae Bank, University of Las Palmas of Gran Canaria, 35214 Telde, Las Palmas, Canary Islands, Spain.*

^e*Single Crystal X-ray Diffraction Laboratory, Interdepartmental Research Service (SIIdI), University Autónoma of Madrid. Cantoblanco, 28049 Madrid, Spain.*

***Corresponding authors**

*E-mail addresses: luis.apaza@uam.es; lnapaza@ucm.es (Luis Apaza T.).
montsetaod@gmail.com (Montserrat Ortega D.).*

ABSTRACT

Three carbamidocyclophanes, A, F and V, and carbamidocylindrofridin A were isolated from the cultured freshwater cyanobacterium *Cylindrospermum stagnale*, collected in the Canary Islands. The chemical structures of these compounds were elucidated through NMR, HRMS and ECD spectroscopy. The absolute configuration of carbamidocyclophane A was confirmed using X-ray-diffraction. All compounds showed apoptotic capacity against the SK-MEL-1, SK-MEL-28 and SK-MEL-31 tumour cells. Carbamidocylindrofridin A had the highest anti-tumour potential, with an IC₅₀ of 1±0.3 µM in the SK-MEL-1 cell line.

Keywords:

Cylindrospermum stagnale, Nostocaceae, Cyanobacterium, anti-tumour, carbamidocyclophane, carbamidocylindrofridin

1. Introduction

Cyanobacteria (blue-green algae) are a group of photosynthetic prokaryotes, with an oxygenic photosynthesis similar to plants (Adams & Duggan, 1999) and a cellular organisation similar to that of gram-negative bacteria (Stanier, 1988). Cyanobacteria have been considered an important source of structurally diverse and biologically active natural constituents such as: alkaloids, sesterterpenoids, peptides, polyketides, porphyrins, terpenoids and volatile alkanes (Nunnery et al., 2010; Cabanillas et al., 2018; Singh et al., 2020). The diversity of their specialised metabolites is due to the ability of cyanobacteria to combine genes encoding nonribosomal peptide synthetases (NRPS) and polyketide synthases (PKSs) through enzymatic reactions such as methylations, oxidations, reductions and other chemicals modifications (Gademann & Portmann, 2008; Welker, 2008).

Compounds isolated from cyanobacteria have shown a wide range of biological properties that include anti-inflammatory (Malloy et al., 2011; Tabarza et al., 2020), anti-leukemic (Humisto et al., 2016), neurotoxic (Soria-Mercado et al., 2009), and anti-tumour effects (Han et al., 2006). In this context, the anti-tumour potential of cyanobacteria has been the most promising, with IC₅₀ values in the low nanomolar range (Mooberry et al., 2003; Sielaff et al., 2006; Tan, 2007).

In our study on cyanobacteria, we have researched the chemistry and biology of the *Cylindrospermum stagnale* BEA 0605B species (Garajonay National Park, Canary Islands, Spain). This species of cyanobacteria has been shown to be a source of diverse bioactive compounds such as [7.7] paracyclophanes, alkylresorcinols, cylindrofridins and

121
122
123 69 dihydroanatoxins that had a strong anti-tumour effect (IC_{50} in the low micromolar range) in
124
125 70 different human cancer cell lines (Kang et al., 2012; Preisitsch et al., 2015; Méjean et al.,
126
127 71 2016; May et al., 2017; Ganesan et al., 2020). Herein we report the isolation of the known
128
129 72 carbamidocyclophanes A and F, and of the unknown carbamidocyclophane V and
130
131 73 carbamidocylindrofridin A. Their anti-tumour potential has been tested in the SK-MEL-1,
132
133 74 SK-MEL-28 and SK-MEL-31 cell lines, while using a control non-tumour cell line (PBMCs).
134
135 75

136 76 **2. Results and discussion**

137 77 *2.1 Isolation and structural determination of specialised metabolites*

138 78
139 79 The lyophilised biomass (8 g) of *C. stagnale* was extracted by repeated maceration with
140
141 80 $CH_2Cl_2/MeOH$ (1:1). The dichloromethane/methanol extract (2.10 g) was successively
142
143 81 fractionated with AcOEt and $CH_2Cl_2/MeOH$ to produce four specialised metabolites. Based
144
145 82 on spectroscopic and spectrometric data, as well as reported values from the literature, we
146
147 83 could identify carbamidocyclophane A (**1**), of unknown absolute configuration (Bui et al.,
148
149 84 2007), and carbamidocyclophane F (**2**) (Luo et al., 2014) (Figure 1).
150
151 85

152 86
153 87
154 88
155 89
156 90
157 91
158 92
159 93
160 94
161 95
162 96
163 97
164 98
165 99
166 100
167 101
168 102
169
170
171
172
173
174
175
176
177
178
179
180

Figure 1.

154 88 The absolute configuration of carbamidocyclophane A (**1**) was established by X-ray
155 89 analysis, obtaining an individual crystal from an acetone/ethyl acetate solution. Its structure
156 90 was described using the SCXRD data (Figure 2). This compound co-crystallised with several
157 91 interstitial solvent molecules (acetone and ethyl acetate) in the chiral monoclinic $P2_1$ space
158 92 group. Each molecule of carbamidocyclophane A established four O-H \cdots O bonds with four
159 93 adjacent solvent molecules (two acetone and two ethyl acetate) through the four hydroxyl
160 94 groups. Additionally, each molecule of carbamidocyclophane A was bonded with other two
161 95 neighbouring carbamidocyclophane molecules by N-H \cdots O bonds to yield infinite chains of
162 96 molecules in the *b* direction (Figure 3S and Table 3S). Regarding the molecular structure of
163 97 carbamidocyclophane A, one of the lateral chains is heavily disordered and only the most
164 98 occupied positions of atoms C14, C15, Cl3 and Cl4 could be located (50% of the
165 99 corresponding electron density, labelled as C14A, C15A, Cl3A and Cl4A). Finally, an
166 100 additional maximum was found in the electron density map (Cl3B) and was included in the
167 101 model as an alternative position of Cl3, accounting for a supplementary 25% of the
168 102 corresponding electron density. About the disorder, we tried to refine anisotropically the less

populated location in the Cl3 model (Cl3B), but the electron density for this position was very small and the overall model did not improve.

Figure 2.

Concerning the absolute configuration, we used SCXRD and performed the calculations to obtain the Hooft parameter with PLATON (Spek, 2009). The resulting value was $y=0.082$ (19), with a probability of $0.00E+00$ that the structure was inverted (correlation coefficient=1.000). The absolute configuration of the six stereogenic carbons in carbamidocyclophane A was: *5R*, *10S*, *11R*, *18R*, *23S* and *24R* (see figure 4S for the labelling scheme). This could be readily identified due to the anomalous dispersion of the chlorine atoms.

Compound **3** was obtained as a white amorphous powder. HRESIMS confirmed the molecular formula of $C_{37}H_{53}NO_6Cl_4$ based on its sodium adduct with m/z of 770.2521 $[M+Na]^+$ (calcd. for $C_{37}H_{53}NNaO_6Cl_4$, 770.2519), suggesting ten degrees of unsaturation. The NMR data (Table 1) showed similarities to the spectrum of compound **1**, and thus confirmed the presence of a tetrachlorinated [7.7] paracyclophane skeleton. Moreover, compound **3** showed two sets of resonances, similar to compound **2**, thus suggesting an asymmetrical substituent pattern.

Table 1.

The analysis of the 1H NMR spectrum of compound **3** revealed signals of aromatic protons [δ_H 6.00 (s, H-25), 6.03 (s, H-23), 6.13 (s, H-12) and 6.21 (s, H-10)], two dichlorinated methines [δ_H 5.83 (t, $J=6.2$ Hz, H-30 and H-34)] (Hawkes et al., 1974), one oxymethine signal at δ_H 4.83 (d, $J=10.0$ Hz, H-14) similar to compound **1** (H-1/H-14), two benzylmethine at δ_H 3.20 (m, H-7 and H-20), two methyl groups at δ_H 0.94 (d, $J=6.5$ Hz, H-35) and δ_H 0.99 (d, $J=6.5$ Hz, H-36), and methylene proton signals at a δ_H between 0.60 and 2.20. Moreover, the 1H NMR spectrum helped us to identify a methylene group at δ_H 1.83 (t, $J=13.0$ Hz, H-1_a) and δ_H 2.60 (dd, $J=13.0$ and 3.7 Hz, H-1_b). Thus, compared to compound **1**, compound **3** has lost the carbamate group at the C-1 position. Analysing the ^{13}C NMR spectrum, only one signal corresponding to the carbamate group (C-37) at δ_C 159.8 and a signal corresponding to the oxymethine (C-14) at δ_C 83.5 were observed. Finally, a methylene group was observed at δ_C 45.8, correlated by HMQC with H-1_a and H-1_b.

Confirmation of the loss of the carbamate group was obtained by HMBC correlation of H-1 with the aromatic methines C-23 and C-25, as well as with the methyls C-35 and C-2.

The relative configuration of compound **3** was confirmed based on the NOESY spectrum. Since the coupling constant had a value of $J=10.0$ Hz between H-14 and H-15, the relative configuration was assigned as *anti*, showing the same stereo configuration as the natural carbamidocyclophanes (Bui et al., 2007; Luo et al., 2014). Due to biosynthetic considerations (Preisitsch et al., 2016), it was determined that compound **3** has an identical configuration to compound **1**, as showed by the crystallographic data and the in-depth study carried out by Nakamura et al. (2017). This study argued that only macrocycling can take place at the C-2 (*S*) and C-7 (*R*) position. This data confirms that the absolute configuration of the carbons is: 2*S*, 7*R*, 14*R*, 15*S* and 20*R*. Thus, taking into account all the analytical data, compound **3** was identified as carbamidocyclophane V (Figure 3), a congener of compounds **1** and **2**.

Figure 3.

The HRESIMS spectrum of compound **4** showed an $[M+Na]^+$ ion with m/z of 865.2290, corresponding to the molecular formula of $C_{38}H_{55}N_2O_8Cl_5$ (calcd. for $C_{38}H_{55}N_2NaO_8Cl_5$, 865.2293), suggesting ten degrees of unsaturation (Table 2).

Table 2.

The analysis of the 1H NMR data showed a triplet at δ_H 6.15 (t, $J=2.1$ Hz, H-34) with an integral corresponding to one proton, but no additional signal corresponding to an aromatic proton, revealing a 1,3,5-trisubstitution pattern in one of the two aromatic systems. This data suggests the opening of the [7.7] paracyclophane ring. Each terminal position of the two alkyl chains showed two bearing chlorine atoms, at δ_H 5.99 (t, 1H, $J=6$ Hz, H-1), δ_C 74.8 (C-1), δ_H 5.82 (t, 1H, $J=6$ Hz, H-20) and δ_C 75.4 (C-20). Moreover, two oxymethine doublets at δ_H 5.27 (d, 1H, $J=5.7$ Hz, H-11) and 5.23 (d, 1H, $J=6.4$ Hz, H-30), and δ_C 80.6 and 80.9 were observed. These chemical shifts are characteristics of oxymethines bonded to carbamoyl groups.

In the 1H NMR spectrum, only one signal of the characteristic CH bridge of paracyclophanes was observed at δ_H 3.22 (m, 1H, H-24). By HSQC, a correlation was established between H-multiplet (δ_H 3.89; m, 1H, H-5) and δ_C 64.5 (C-5), confirming that a

chlorine atom is located within the aliphatic chain. The ^1H - ^1H COSY spectrum allowed the assignment of the two spin systems corresponding to the aliphatic chains of the open macrocycle. The localisation of the chlorine atom at the C-5 position was unambiguously assigned through the HMBC spectrum, showing correlations with H-1, H-4 and H-6. H-10 was correlated with methyl moiety H-18 by ^1H - ^1H COSY. The methine (H-11) showed a correlation with a CH (C-13) of the benzene ring and with a carbamoyl moiety (C-19). In the second spin system corresponding to the aliphatic chain, a substitution was observed at the C-24, C-30 and C-31 positions. The HMBC spectrum displayed a $^{2,3}J_{\text{CH}}$ correlation between H-30 and C-38, confirming the second carbamoyl moiety. The HMBC data confirmed the presence of the 1,3,5-trisubstituted ring through a $^{2,3}J_{\text{CH}}$ correlation between H-34 and C-33/C-35, and H-36 and C-35. The connection between the two aliphatic chains that determines the opening of the macrocycle was confirmed through HMBC due to the following bidirectional correlations: $^{2,3}J_{\text{CH}}$ H-13/C-11, $^{2,3}J_{\text{CH}}$ H-13/C-15 and $^{2,3}J_{\text{CH}}$ H-24/C-15.

The absolute configuration was established based on the relative configuration from ECD and the results from the biosynthetic study carried out by Nakamura et al. (2017). In the electronic circular dichroism (ECD) spectrum, a positive Cotton effect was observed at 223 nm ($\Delta\epsilon = +2.18$) and a negative Cotton effect at 278.1 nm ($\Delta\epsilon = -1.15$). The spectra were very similar to those of the cylindrofridins (Preisitsch et al., 2016). In contrast to the rigid carbamidocyclophanes, the linear scaffold showed greater conformational flexibility. Therefore, the $^3J_{\text{H-11, H-10}}$ could not be used to establish the relative configurations. However, Nakamura et al. (2017) have shown that the macrocyclization process occurs when position 5 (chlorine) has an *R* configuration, and positions 10 and 29 have an *S* configuration. In addition, the position 24 needs to have an *S* configuration, and positions 11 and 30 need to have an *R* configuration. Therefore, based on this study and the ECD data, the proposed configuration is presented in Figure 3. These results confirm the structure suggested by the HRMS data, and the compound **4** is carbamidocylindrofridin A (Figure 4).

Figure 4.

2.2 Biological assays

All compounds showed cytotoxicity in the three tumour cell lines. This effect was especially high for carbamidocylindrofridin A. Through the XTT assay, we obtained CC_{50}

values of $4.6 \pm 0.3 \mu\text{M}$ (SK-MEL-1), $10.1 \pm 0.3 \mu\text{M}$ (SK-MEL-28) and $8.8 \pm 0.2 \mu\text{M}$ (SK-MEL-31), while the positive control (Actinomycin D) had a CC_{50} of $0.05 \pm 0.01 \mu\text{M}$ (Table 3).

Table 3.

The XTT assay is based on the determination of intracellular NAD (P)-dependent oxidoreductase activities, measuring mainly dehydrogenases that reduce XTT (Roehm et al., 1991). Dehydrogenases are found in the matrix of the mitochondria (Wang et al., 2011). All the compounds, in particular carbamidocylindrofridin A, caused a rapid depolarisation of the mitochondrial membrane and the suppression of respiration due to the consumption of NADH which ultimately led to apoptosis (cell death).

To study compound-induced cell death, cells were treated using the four compounds at different concentrations. Subsequently, cells were treated with a combination of Rhodamine 123 and PI staining as an apoptotic-necrotic cell marker, and then analysed by flow cytometry (Hosseini-Pirdehi et al., 2019; Qu et al., 2019). The data showed that all the compounds have anti-tumour potential. The apoptotic effect of carbamidocylindrofridin A was higher than the effect of the other compounds with an IC_{50} of $1 \pm 0.3 \mu\text{M}$ (SK-MEL-1), $2.6 \pm 0.3 \mu\text{M}$ (SK-MEL-28) and $2 \pm 0.3 \mu\text{M}$ (SK-MEL-31), and this compound is the only compound with a similar anti-tumour effect to the positive control ($\text{IC}_{50} = 0.05 \pm 0.01 \mu\text{M}$) ($^{\text{ns}}p > 0.999$).

Table 4.

The selection of the positive control (Actinomycin D) was based on its structural similarity to carbamidocyclophanes and carbamidocylindrofridins. The apoptotic mechanism of actinomycin D is due to the binding of its phenoxazone ring to DNA regions rich in 5'-GpC-3', and to the stabilisation of its cleavable complexes (topoisomerases I and II) through the polypeptide rings of the carbamoyl groups (Wu & Yung, 1994; Lohani et al., 2016). Carbamidocylindrofridin A binds to the 5'-GpC-3' regions in the DNA duplex through its dihydroxylated aromatic rings; the alkyl chains, that have chlorine atoms, and the carbamoyl groups stabilise the cleavable complexes of topoisomerases I and II.

3. Conclusion

In this report, we have analysed carbamidocyclophanes and carbamidocylindrofridins that we isolated for the first time from the cyanobacterium *C. stagnale*. Only carbamidocyclophane V and carbamidocylindrofridin A showed anti-tumour activity at micromolar concentrations, despite having minimal effects on normal cells. These findings indicate that these compounds can be promising lead molecules for the development of new anti-tumour drugs. This is in addition to their use as antimicrobials, antifungals, antivirals, enzyme inhibitors, and even immunosuppressants (Bui et al., 2007; Preisitsch et al., 2014; Singh et al., 2017).

4. Experimental section

4.1. General experimental procedures

First grade organic solvents were used for isolating the compounds. The solvents were purchased from Sigma-Aldrich. TLC (Thin-layer chromatography) was performed using Merck Silica gel 60-F₂₅₄ plates. Chromatograms thus obtained were visualised by UV absorbance (254 nm) and through heating a plate stained with phosphomolybdic acid. Manual chromatography column was performed with silica gel (40-63 μm and 20-45 μm , Merck) and the indicated eluent was used in accordance with standard techniques.

NMR experiments were performed using a Bruker Avance DRX 500 spectrometer operating at 500 MHz (¹H) or 125 MHz (¹³C). The deuterated solvent was methanol-*d*₄. Spectra were calibrated by assigning the residual solvent peak at δ_{H} 3.31 and δ_{C} 49.0 for methanol-*d*₄. HREIMS analyses were performed using a QSTAR XL quadrupole TOF mass spectrometer. MS samples were prepared in MeOH. Single crystal X-ray crystallographic data was used for the structural elucidation of carbamidocyclophane A, and this data was obtained at 200(2) K from a Bruker Kappa Apex II diffractometer equipped with Mo anode. Information about crystal and refinement data can be found in the supporting information. The crystallographic data has been deposited at the Cambridge Crystallographic Data Centre (CCDC, 1969832) and can be obtained free of charge via www.ccdc.cam.ac.uk/data_request/cif. Molecular graphics were produced with Mercury 4.2.0.

4.2. Biological material

The cyanobacterium *C. stagnale* (GTBC-360) of the family Nostocaceae was isolated from a sample collected in the Garajonay National Park, La Gomera, Gran Canaria (Canary Islands, 28°07'40.7"N and 17°14'12.6"W, Spain). The 16S ribosomal RNA gene sequence was deposited in the GenBank (accession no. MN845140.1). The remaining sample was grown under axenic conditions by Valoralia I más D. The cyanobacteria were cultivated in 2 L flasks containing BG-110 medium. The cultures were grown by bubbling with air, and were incubated at 23±1°C, illuminated exclusively with ambient light. Subsequently, the cultures were harvested after 21 days, and the biomass was collected by centrifugation and finally lyophilised.

4.3. Extraction and isolation

The lyophilised biomass (8 g) was extracted by repeated maceration with CH₂Cl₂/MeOH (1:1, 3x1 L). The biological activity of the dichloromethane/methanol extract (2.60 g) was performed (cytotoxicity and apoptotic capacity), showing a relevant activity against all tumour cell lines.

The dichloromethane/methanol extract (2.10 g) was fractionated in a vacuum column chromatography (12x60 cm) with silica gel (40-63 µm), using as mobile phase a gradient that started with AcOEt (3 L), followed by CH₂Cl₂/MeOH (15:1, 3 L) and ended with CH₂Cl₂/MeOH (5:1, 3 L) to produce five fractions (A-E). Fraction A (765 mg) was found to be the most active fraction (apoptotic capacity).

Finally, fraction A (715 mg) was subjected to separation by silica gel (20-45 µm) column (8x30 cm) chromatography, using as eluent hept-AcOEt (3:1, 3 L) and hept-AcOEt (1:1, 3 L), obtaining six fractions. Fractions **1** (200 mg), **2** (17 mg), **3** (10 mg) and **4** (15 mg) resulted in pure compounds, identifying them as: carbamidocyclophane A (**1**), carbamidocyclophane F (**2**), carbamidocyclophane V (**3**) and carbamidocylindrofridin A (**4**).

4.4. Spectroscopic data

4.4.1. Carbamidocyclophane A (**1**)

White amorphous powder; $[\alpha]_D^{22}$ -1 (*c* 0.4, MeOH); ¹H NMR (500 MHz, CD₃OD): δ_H 4.83 (d, 2H, *J*=9.6 Hz, H-1/H-14), 1.76-1.68 (m, 2H, H-2/H-15), 0.79 (m, 2H, H-3a/H-16a), 0.68 (m, 2H, H-3b/H-16b), 1.44 (m, 2H, H-4a/H-17a), 0.86 (m, 2H, H-4b/H-17b), 0.95 (m,

2H, H-5a/H-18a), 0.74 (m, 2H, H-5b/H-18b), 2.06 (m, 2H, H-6a/H-19a), 1.34 (m, 2H, H-6b/H-19b), 3.23 (m, 2H, H-7/H-20), 6.20 (s, 2H, H-10/H-23), 6.14 (s, 2H, H-12/H-25), 2.04 (m, 2H, H-27a/H-31a), 1.54 (m, 2H, H-27/H-31), 1.37 (m, 4H, H-28/H-32), 2.16 (m, 2H, H-29a/H-33a), 2.09 (m, 2H, H-29b/H-33b), 5.82 (t, 1H, $J=5.6$ Hz, H-30/H-34), 1.00 (d, 6H, $J=6.4$ Hz, H-35/H-36). ^{13}C NMR (125 MHz, CD_3OD): δ_{C} 83.5 (C-1/C-14), 40.4 (C-2/C-15), 34.5 (C-3/C-16), 29.6 (C-4/C-17), 30.4 (C-15/C-18), 35.3 (C-6/C-19), 36.4 (C-7/C-20), 117.3 (C-8/C-21), 158.8 (C-9/C-22), 105.2 (C-10/C-23), 140.1 (C-11/C-24), 109.4 (C-12/C-25), 157.0 (C-13/C-26), 33.7 (C-27/C-31), 25.8 (C-28/C-32), 45.1 (C-29/C-33), 75.3 (C-30/C-34), 156.4 (C-37/C-38), 16.6 (C-35/C-36); HRESIMS m/z 829.2523 $[\text{M}+\text{Na}]^+$ (calcd. for $\text{C}_{38}\text{H}_{54}\text{N}_2\text{O}_8\text{NaCl}_4$, 806.2523).

4.4.2. Carbamidocyclophane F (2)

White amorphous powder; $[\alpha]_D^{22}$ -3 (c 0.2, MeOH); ^1H NMR (300 MHz, CD_3OD): δ_{H} 3.75 (d, 1H, $J=9.6$ Hz, H-1), 1.55 (m, 1H, H-2), 0.63 (m, 1H, H-3a), 0.74 (m, 1H, H-3b), 1.44 (m, 2H, H-4a/H-17a), 0.83 (m, 2H, H-4b/H-17b), 0.95 (m, 2H, H-5a/H-18a), 0.72 (m, 2H, H-5b/H-18b), 1.33 (m, 4H, H-6/H-19), 3.20 (m, 2H, H-7/H-20), 6.21 (br, 1H, H-10), 6.13 (br, 1H, H-12), 4.81 (d, 1H, $J=10.3$ Hz, H-14), 1.73 (m, 1H, H-15), 0.71 (m, 1H, H-16a), 0.79 (m, 1H, H-16b), 6.25 (s, 1H, H-23), 6.08 (s, 1H, H-25), 1.51 (m, 2H, H-27a/H-31a), 2.04 (m, 2H, H-27b/H-31b), 1.36 (m, 4H, H-28/H-32), 2.06 (m, 2H, H-29a/H-33a), 2.20 (m, 2H, H-29b/H-33b), 5.82 (t, 2H, $J=6.2$ Hz, H-30a/H-34a), 5.83 (t, 2H, $J=6.2$ Hz, H-30b/H-34b), 1.06 (d, 3H, $J=6.5$ Hz, H-35), 1.00 (d, 3H, $J=6.5$ Hz, H-36), ^{13}C NMR (75 MHz, CD_3OD): δ_{C} 81.7 (C-1), 42.0 (C-3), 35.2 (C-4/C-17), 29.7 (C-4), 29.8 (C-17), 30.5 (C-5), 30.6 (C-18), 35.3 (C-6/C-19), 36.3 (C-7), 36.4 (C-20), 117.4 (C-8), 158.8 (C-9), 105.2 (C-10), 140.1 (C-11), 109.4 (C-12), 157.0 (C-13), 83.5 (C-14), 40.4 (C-15), 34.5 (C-16), 116.7 (C-21), 158.9 (C-22), 105.0 (C-23), 144.2 (C-24), 108.8 (C-25), 157.1 (C-26), 33.7 (C-27), 33.8 (C-31), 25.7 (C-28), 25.8 (C-32), 45.0 (C-29), 45.2 (C-33), 75.3 (C-30), 75.4 (C-34), 17.0 (C-36), 16.6 (C-35), 159.8 (C-37); HRESIMS m/z 786.2489 $[\text{M}+\text{Na}]^+$ (calcd. for $\text{C}_{37}\text{H}_{53}\text{NO}_7\text{NaCl}_4$, 786.2465).

4.4.3. Carbamidocyclophane V (3)

White amorphous powder; $[\alpha]_D^{22}$ -6 (c 0.3, MeOH); ^1H NMR and ^{13}C NMR, Table 1; HRESIMS m/z 770.2521 $[\text{M}+\text{Na}]^+$ (calcd. for $\text{C}_{37}\text{H}_{53}\text{NO}_7\text{NaCl}_4$, 770.2519).

4.4.4. Carbamidocylindrofridin A (4)

White amorphous powder; $[\alpha]_D^{22} +27$ (c 1.1, MeOH); ^1H NMR and ^{13}C NMR, Table 2; HRESIMS m/z 865.2290 $[\text{M}+\text{Na}]^+$ (calcd. for $\text{C}_{38}\text{H}_{54}\text{N}_2\text{O}_8\text{NaCl}_4$, 865.2293).

4.5. X-ray Crystallographic Data of carbamidocyclophane A (1)

A clear colourless plate-like specimen of carbamidocyclophane A, with approximate dimensions of 0.107 mm x 0.218 mm x 0.493 mm, was used for the X-ray crystallographic analysis. The X-ray intensity was measured using a Bruker Kappa Apex II diffractometer.

The frames were integrated using the Bruker SAINT software package by a narrow-frame algorithm. The integration of the data using a monoclinic unit cell yielded a total of 90850 reflections at a maximum θ angle of 25.35° (0.83 Å resolution); 10751 reflections were independent (average redundancy of 8.450, completeness=100.0%, R_{int} =5.27%, R_{sig} =3.56%) and 8588 (79.88%) were greater than $2\sigma(F^2)$. The final cell constants of $a=9.0920(6)$ Å, $b=35.250(2)$ Å, $c=10.1315(6)$ Å, $\beta=115.077(2)^\circ$, volume=2941.0(3) Å³ were based on the refinement of the XYZ-centroids of 9988 reflections above $20\sigma(I)$ with $5.004^\circ < 2\theta < 44.97^\circ$. Data was corrected for absorption effects using the multi-scan method (SADABS). The ratio of minimum to maximum apparent transmission was 0.931. The calculated minimum and maximum transmission coefficients (based on crystal size) were 0.8960 and 0.9760.

The structure was elucidated and refined using the Bruker SHELXTL Software Package, using the space group $P2_1$, with $Z=2$. The final anisotropic full-matrix least-squares refinement on F^2 with 663 variables converged at $R1=9.55\%$, for the observed data, and $R2=28.45\%$ for all data. The goodness-of-fit was 1.053. The largest peak in the final difference electron density synthesis was 1.144 e⁻/Å³ and the largest hole was -0.613 e⁻/Å³ with an RMS deviation of 0.116 e⁻/Å³. Based on the final model, the calculated density was 1.198 g/cm³ and $F(000)$, 1136 e⁻.

4.6. Cell culture

Three human skin malignant melanoma cell lines were used in this study: SK-MEL-1 (HTB-67), SK-MEL-28 (HTB-72) and SK-MEL-31 (HTB-73). They were obtained from the American Type Culture Collection (ATTC). In addition, PMBCs were used to assess the safety of the compounds. PBMCs from healthy donors were isolated from the blood by Ficoll

(Rafer) density gradient centrifugation in Leucosep tubes (Greiner Bio-One), following the manufacturer's recommendations. All experiments using human PBMCs were approved by the ethics committees of the University Hospital of La Paz, Madrid (No. 913/2018). Cells were cultured in DMEM (Dulbecco's modified eagle medium, Sigma-Aldrich St. Louis, USA) supplemented with L-glutamine (PanReac AppliChem, Barcelona, Spain), 10% FBS (Fetal bovine serum, Summit Biotechnology Ft. Collins, CO), 100 U/mL penicillin and 100 μ g/mL streptomycin (Fisher Scientific, Pittsburgh, USA), at 37°C in hypoxic conditions (1% O₂), thus mimicking the *in vivo* tumour microenvironment.

4.7. Cytotoxic assay

Cells were seeded in 96-well plates at a density of 5×10^4 cells/well and incubated overnight at 37°C in a humidified atmosphere of 5% CO₂. Stock solutions of the samples were prepared by dissolving them in DMSO at a concentration of 20 μ g/mL for the fractions and 10 μ M for the compounds. Subsequently, from the stock solutions, a series of dilutions were made until a final DMSO concentration of 0.1% was obtained in each of the wells of the plate for each of the tested concentrations (Park *et al.*, 1992). The tested concentrations were 100, 50, 25, 12.5, 6.25, 3.13, 1.56, 0.78, 0.39 and 0.20 μ g/mL or μ M.

XTT viability assay-inhibition of H₂O₂-induced cytotoxicity at various concentrations was tested through the method of XTT-formazan (Weislow *et al.*, 1989), using the above-mentioned cell lines. These cells were sown in a 96-well plate and allowed to grow at 37°C. After 12 h, medium was removed from all wells. 200 μ L fresh medium were added to the control wells. Cells in each test well were treated with 0.1 mM H₂O₂ (prepared in medium) along with different concentrations of the samples. Actinomycin D ($\geq 95\%$ Sigma-Aldrich, CAS Number 50-76-0) was used as a positive control at a concentration of 0.01 μ M. Cells in both control and test wells were re-incubated for 12 h, maintaining the same conditions. After the treatment incubation period, medium in each well was substituted by 200 μ L of fresh medium, followed by the addition of 50 μ L of XTT (0.6 mg/mL) containing 25 μ M peroxymonosulfate (PMS). The plate was further incubated for 4 h in the same conditions. Absorbance was measured at 450 nm using a spectrophotometric ELISA plate reader (SpectraMax® i3, Molecular Devices, CA, USA).

4.8. Apoptosis assay

Apoptosis was determined by the rhodamine method. A double staining was used (rhodamine 123 to detect changes in the mitochondrial membrane and propidium iodide to

detect necrotic cells). The cells (20×10^4) were seeded in 55 mm plates with 2 mL of complete DMEM and treated with the compounds at a concentration obtained by the viability assay XTT (CC_{50}). Actinomycin D ($\geq 95\%$ Sigma-Aldrich, CAS Number 50-76-0) was used as a positive control at a concentration of $0.05 \mu\text{M}$. 72 hours after treatment, cells were incubated with $5 \mu\text{L}$ of rhodamine 123 ($1 \mu\text{g}/\mu\text{L}$) for 30 minutes. All cells in each well were harvested and centrifuged at 500 rpm for 10 minutes. The cell pellet was washed 3 times with 1 mL of PBS 1x+1% BSA solution and resuspended in 500 μL of PBS 1x+1% BSA solution, containing $0.5 \mu\text{L}$ of propidium iodide (PI) ($5 \mu\text{g}/\mu\text{L}$). The entire procedure was performed at 4°C . The samples were analysed by flow cytometry, using the BD-FACSCalibur™ cytometer (Becton Dickinson BioScience, San Jose, CA, USA). Expo32 software was used to analyse the data. The percentage of Rho-negative and PI-negative cells corresponded to the apoptotic population.

4.9. Statistical analysis

CC_{50} and IC_{50} values were determined by non-linear regression. All the experiments were performed in triplicate. One-way ANOVA statistical analysis (Tukey's multiple comparisons test, $*p < 0.05$; $***p < 0.001$) was performed to evaluate the differences between values. All the analysis was performed using GraphPad Prism, version 8.4.3.

Conflicts of interest

The authors declare no conflict of interest.

Acknowledgements

This work was supported by the Fundación de la Universidad Autónoma de Madrid (FUAM).

Author contribution

SMC and DFRV contributed to the production of cultures; AMQ contributed to the taxonomic determination; VTP and AHC contributed to the conception and experimental design of the chemical study; LAT and ARS contributed to the analysis of spectral data; JP contributed to the X-ray crystallography analysis; LAT and MOD contributed to the conception and experimental design of the pharmacological study; LAT and ARS contributed to the writing and review of the manuscript.

Supporting Information

¹H and ¹³C NMR, ¹H-¹H COSY, HSQC, HMBC, and HRESIMS spectra for compound **1-4** (Figures 1S-22S) and single crystal X-ray data for compound **1** (Tables 1S-3S).

References

- Adams, D.G., Duggan, P.S., 1999. Heterocyst and akinete differentiation in cyanobacteria. *New Phytol.* 144, 3-33. <https://doi.org/10.1046/j.1469-8137.1999.00505.x>.
- Bui, H.T.N, Jansen, R., Pham, H.T.L, Mundt, S., 2007. Carbamidocyclophanes A-E, chlorinated paracyclophanes with cytotoxic and antibiotic activity from the Vietnamese cyanobacterium *Nostoc* sp. *J. Nat. Prod.* 70, 499-503. <https://doi.org/10.1021/np060324m>.
- Cabanillas, A.H., Tena, P.V., Corral, M.S., Valencia, R.D.F., Quintana, M.A., Doménech, O.M., Sánchez, R.A., 2018. Cybastacines A and B: antibiotic sesterterpenes from *Nostoc* sp. *Cyanobacterium. J. Nat. Prod.* 81, 410-413. <https://doi.org/10.1021/acs.jnatprod.7b00638>.
- Gademann, K., Portmann, C., 2008. Secondary Metabolites from Cyanobacteria: Complex Structures and Powerful Bioactivities. *Curr. Org. Chem.* 12, 326-341. <https://doi.org/10.2174/138527208783743750>.
- Ganesan, V., Raja, R., Hemaiswarya, S., Carvalho, I.S., Anand, N., 2020. Isolation and characterization of two novel plasmids pCYM01 and pCYM02 of *Cylindrospermum stagnale*. *Saudi J. Biol. Sci.* 27(1), 535-542. <https://doi.org/10.1016/j.sjbs.2019.11.017>.
- Han, B., Gross, H., Goeger, D.E., Mooberry, S.L., Gerwick, W.H., 2006. Aurilides B and C, cancer cell toxins from a Papua New Guinea collection of the marine cyanobacterium *Lyngbya majuscula*. *J. Nat. Prod.* 69, 572-575. <https://doi.org/10.1021/np0503911>.
- Hawkes, G.E., Smith, R.A., Roberts, J.D., 1974. Nuclear magnetic resonance spectroscopy. Carbon-13 chemical shifts of chlorinated organic compounds. *J. Org. Chem.* 39, 1276-1290. <https://doi.org/10.1021/jo00923a026>.
- Hosseinjani-Pirdehi, H., Allah Mahmoodi, N.O., Taheri, A., Asalemi, K.A.A., Esmaeili, R., 2019. Selective immediate detection of Cu²⁺ by a pH-sensitive rhodamine-based fluorescence probe in breast cancer cell-line. *Spectrochim Acta A Mol Biomol Spectrosc.* 229, 117989. <https://doi.org/10.1016/j.saa.2019.117989>.

- Humisto, A., Herfindal, L., Jokela, J., Karkman, A., Bjørnstad, R., Choudhury, R.R., Sivonen, K., 2016. Cyanobacteria as a Source for Novel Anti-Leukemic Compounds. *Curr Pharm Biotechnol.* 17(1), 78-91. <https://doi.org/10.2174/1389201016666150826121124>.
- Kang, H.S., Santarsiero, B.D., Kim, H., Kronic, A., Shen, Q., Swanson, S.M., Chai, H., Kinghorn, A.D., Orjala, J., 2012. Merocyclophanes A and B, antiproliferative cyclophanes from the cultured terrestrial Cyanobacterium *Nostoc* sp. *Phytochemistry.* 79, 109. <https://doi.org/10.1016/j.phytochem.2012.03.005>.
- Lohani, N., Singh, H.N., Moganty, R.R., 2016. Structural aspects of the interaction of anticancer drug Actinomycin-D to the GC rich region of *hmgbl* gene. *Int. J. Biol. Macromol.* 87, 433-442. <https://doi.org/10.1016/j.ijbiomac.2016.02.060>.
- Luo, S., Kang, H.S., Kronic, A., Chlipala, G.E., Cai, G., Chen, W.L., Franzblau, S.G., Swanson, S.M., Orjala, J., 2014. Carbamidocyclophanes F and G with Anti-*Mycobacterium tuberculosis* Activity from the Cultured Freshwater Cyanobacterium *Nostoc* sp. *Tetrahedron Lett.* 55, 686-689. <https://doi.org/10.1016/j.tetlet.2013.11.112>.
- Malloy, K.L., Villa, F.A., Engene, N., Matainaho, T., Gerwick, L., Gerwick, W.H., 2011. Malyngamide 2, an oxidized lipopeptide with nitric oxide inhibiting activity from a Papua New Guinea marine cyanobacterium. *J. Nat. Prod.* 74, 95-98. <https://doi.org/10.1021/np1005407>.
- May, D.S., Chen, W.L., Lantvit, D.D., Zhang, X., Kronic, A., Burdette, J.E., Eustaquio, A., Orjala, J., 2017. Merocyclophanes C and D from the Cultured Freshwater Cyanobacterium *Nostoc* sp. (UIC 10110). *J. Nat. Prod.* 80, 1073-1080. <https://doi.org/10.1021/acs.jnatprod.6b01175>.
- Méjean, A., Dalle, K., Paci, G., Bouchonnet, S., Mann, S., Pichon, V., Ploux, O., 2016. Dihydroanatoxin-a Is Biosynthesized from Proline in *Cylindrospermum stagnale* PCC 7417: Isotopic Incorporation Experiments and Mass Spectrometry Analysis. *J. Nat. Prod.* 79(7), 1775-1782. <https://doi.org/10.1021/acs.jnatprod.6b00189>.
- Mooberry, S.L., Leal, R.M., Tinley, T.L., Luesch, H., Moore, R.E., Corbett, T.H., 2003. The molecular pharmacology of symplostatin 1: A new antimitotic dolastatin 10 analog. *Int. J. Cancer.* 104, 512-521. <https://doi.org/10.1002/ijc.10982>.
- Nakamura, H., Schultz, E.E., Balskus, E.P., 2017. A new strategy for aromatic ring alkylation in cylindrocyclophane biosynthesis. *Nat. Chem. Biol.* 13, 916-921. <https://doi.org/10.1038/nchembio.2421>.

- 504 Nunnery, J.K., Mevers, E., Gerwick, W.H., 2010. Biologically active secondary metabolites
505 from marine cyanobacteria. *Curr. Opin. Biotechnol.* 21, 787-793.
506 <https://doi.org/10.1016/j.copbio.2010.09.019>.
- 507 Park, C.H., Martinez, B.C., 1992. Enhanced release of rosmarinic acid from *Coleus blumei*
508 permeabilized by dimethyl sulfoxide (DMSO) while preserving cell viability and growth.
509 *Biotechnol. Bioeng.* 40, 459-464. <https://doi.org/10.1002/bit.260400403>.
- 510 Preisitsch, M., Harmrolfs, K., Pham, H.T., Heiden, S.E., Füssel, A., Wiesner, C., Pretsch, A.,
511 Swiatecka-Hagenbruch, M., Niedermeyer, T.H.J., Müller, R., Mundt, S., 2014. Anti-
512 MRSA-acting carbamidocyclophanes H-L from the Vietnamese cyanobacterium *Nostoc*
513 sp. CAVN2. *J. Antibiot. Res.* 68, 165-177. <https://doi.org/10.1038/ja.2014.118>.
- 514 Preisitsch, M., Heiden, S.E., Beerbaum, M., Niedermeyer, T.H., Schneefeld, M., Herrmann,
515 J., Kumpfmüller, J., Thürmer, A., Neidhardt, I., Wiesner, C., Daniel, R., Müller, R.,
516 Bange, F.C., Schmieder, P., Schweder, T., Mundt, S., 2016. Effects of Halide Ions on the
517 Carbamidocyclophane Biosynthesis in *Nostoc* sp. CAVN2. *Mar. Drugs.* 14, 1-30.
518 <https://doi.org/10.3390/md14010021>.
- 519 Preisitsch, M., Niedermeyer, T.H., Heiden, S.E., Neidhardt, I., Kumpfmüller, J., Wurster, M.,
520 Harmrolfs, K., Wiesner, C., Enke, H., Müller, R., Mundt, S., 2015. Cyindrofridins A-C,
521 Linear Cyindrocyclophane-Related Alkylresorcinols from the Cyanobacterium
522 *Cylindrospermum stagnale*. *J. Nat. Prod.* 79, 106-115.
523 <https://doi.org/10.1021/acs.jnatprod.5b00768>.
- 524 Qu, X., Yuan, F., He, Z., Mai, Y., Gao, J., Li, X., Yang, D., Cao, Y., Li, X., Yuan, Z., 2019.
525 A rhodamine-based single-molecular theranostic agent for multiple-functionality tumor
526 therapy. *Dyes and Pigments.* 166, 72-83. <https://doi.org/10.1016/j.dyepig.2019.03.009>.
- 527 Roehm, N.W., Rodgers, G.H., Hatfield, S.M., Glasebrook, A.L., 1991. An improved
528 colorimetric assay for cell proliferation and viability utilizing the tetrazolium salt XTT. *J.*
529 *Immunol. Methods.* 142, 257-265. [https://doi.org/10.1016/0022-1759\(91\)90114-u](https://doi.org/10.1016/0022-1759(91)90114-u).
- 530 Sielaff, H., Christiansen, G., Schwecke, T., 2006. Natural products from cyanobacteria:
531 Exploiting a new source for drug discovery. *IDrugs.* 9, 119-127.
- 532 Singh, D.K., Pathak, J., Pandey, A., Singh, V., Ahmed, H., Rajneesh, Kumar D., Sinha, R.P.,
533 2020. Ultraviolet-screening compound mycosporine-like amino acids in cyanobacteria:
534 biosynthesis, functions, and applications. *Advances in Cyanobacterial Biology.* 219-233.
535 <https://doi.org/10.1016/B978-0-12-819311-2.00015-2>.

- Singh, J., Mishra, S.K., Dwivedi, N., 2017. Antibacterial activity of two soil cyanobacteria *Nostoc polludosum* and *Cylindrospermum licheniforme*. J. Algal Biomass Utiln. 8(4), 18-22.
- Soria-Mercado, I.E., Pereira, A., Cao, Z., Murray, T.F., Gerwick, W.H., 2009. Alotamide A, a novel neuropharmacological agent from the marine cyanobacterium *Lyngbya bouillonii*. Org. Lett. 11, 4704-4707. <https://doi.org/10.1021/ol901438b>.
- Spek, L.A., 2009. Structure validation in chemical crystallography. Acta Crystallogr., Sect. D: Biol. Crystallogr. 65, 148-155. <https://doi.org/10.1107/S090744490804362X>.
- Stanier (Cohen-Bazire), G., 1988. Fine structure of cyanobacteria. Methods Enzymol. 167, 157-172. [https://doi.org/10.1016/0076-6879\(88\)67017-0](https://doi.org/10.1016/0076-6879(88)67017-0).
- Tabarzad, M., Atabaki, V., Hosseinabadi, T., 2020. Anti-inflammatory Activity of Bioactive Compounds from Microalgae and Cyanobacteria by Focusing on the Mechanisms of Action. Mol. Biol. Rep. 47(8), 6193-6205. <https://doi.org/10.1007/s11033-020-05562-9>.
- Tan, L.T., 2007. Bioactive natural products from marine cyanobacteria for drug discovery. Phytochemistry. 68, 954-979. <https://doi.org/10.1016/j.phytochem.2007.01.012>.
- Wang, S., Yu, H., Wickliffe, J.K., 2011. Limitation of the MTT and XTT assays for measuring cell viability due to superoxide formation induced by nano-scale TiO₂. Toxicol. in Vitro. 25, 2147-2151. <https://doi.org/10.1016/j.tiv.2011.07.007>.
- Weislow, O.S., Kiser, R., Fine, D.L., Bader, J., Shoemaker, R.H., Boyd, M.R., 1989. New soluble-formazan assay for HIV-1 cytopathic effects: application to high-flux screening of synthetic and natural products for AIDS-antiviral activity. J. Nat. Cancer Inst. 81, 577-586. <https://doi.org/10.1093/jnci/81.8.577>.
- Welker, M., 2008. Cyanobacterial Hepatotoxins: Chemistry, Biosynthesis, and Occurrence. In Seafood and Freshwater Toxins Pharmacology, Physiology and Detection; Botana, L.M., Taylor & Francis Group Boca Raton, FL, USA. pp. 825-843.
- Wu, M.H., Yung, B.Y.M., 1994. Cell cycle phase-dependent cytotoxicity of actinomycin D in HeLa cells. Eur. J. Pharmacol.: Environ. Toxicol. Pharmacol. 270, 203-212. [https://doi.org/10.1016/0926-6917\(94\)90064-7](https://doi.org/10.1016/0926-6917(94)90064-7).

SUPPLEMENTARY FILE

Antitumoral potential of carbamidocyclophanes and carbamidocylindrofridin A isolated from the cyanobacterium *Cylindrospermum stagnale* BEA 0605B

Víctor Tena Pérez^a, Luis Apaza Ticona^{a,b,*}, Alfredo H. Cabanillas^a, Santiago Maderuelo Corral^c, Josefina Perles^e, Diego Fernando Rosero Valencia^c, Antera Martel Quintana^d, Montserrat Ortega Domenech^{c,*}, Ángel Rumbero Sánchez^a

Affiliation

^a*Department of Organic Chemistry, Faculty of Sciences, University Autónoma of Madrid. Cantoblanco, 28049 Madrid, Spain*

^b*Department of Pharmacology, Pharmacognosy and Botany, Faculty of Pharmacy, University Complutense of Madrid. Ciudad Universitaria s/n, 28040 Madrid, Spain*

^c*Valoralia I más D SLU, Tres Cantos, 28760 Madrid, Spain.*

^d*Spanish Algae Bank, University of Las Palmas of Gran Canaria, 35214 Telde, Las Palmas, Canary Islands, Spain.*

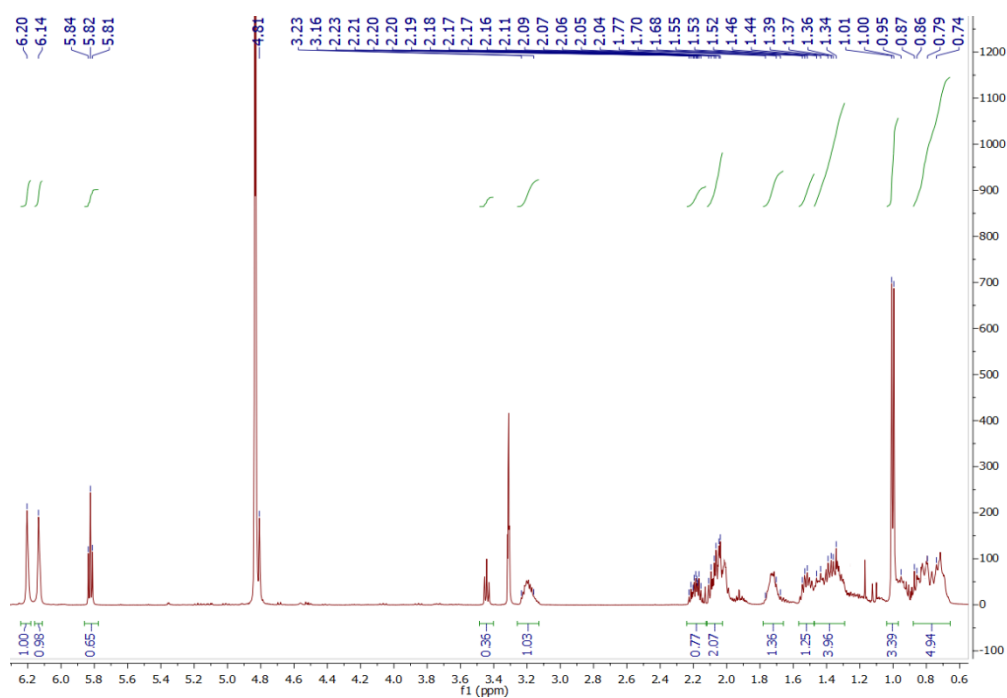
^e*Single Crystal X-ray Diffraction Laboratory, Interdepartmental Research Service (SIIdI), University Autónoma of Madrid Cantoblanco, 28049 Madrid, Spain.*

*Corresponding author

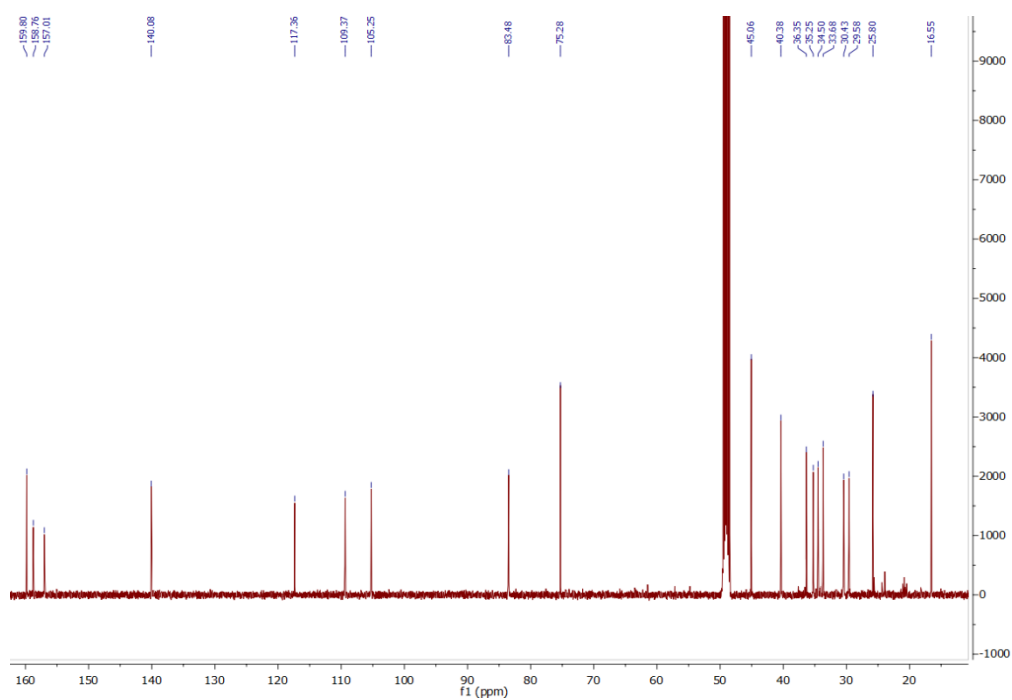
E-mail addresses: luis.apaza@uam.es; lnapaza@ucm.es (Luis Apaza T.).
montsetaod@gmail.com (Montserrat Ortega D.).

Table of contents:

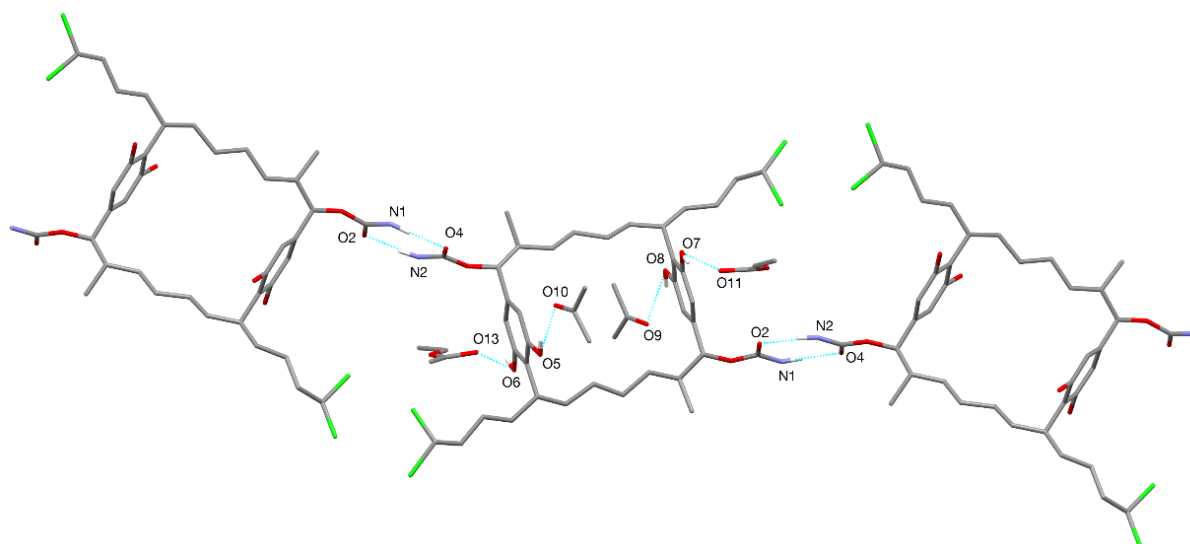
- Figure 1S. ^1H -NMR spectrum of carbamidocyclophane A (1)
- Figure 2S. ^{13}C -NMR spectrum of carbamidocyclophane A (1)
- Figure 3S. Hydrogen bonds found in carbamidocyclophane A (1)
- Figure 4S. Labelled molecule of carbamidocyclophane A (1)
- Figure 5S. HRESIMS spectrum of carbamidocyclophane A (1)
- Figure 6S. ^1H -NMR spectrum of carbamidocyclophane F (2)
- Figure 7S. ^{13}C -NMR spectrum of carbamidocyclophane F (2)
- Figure 8S. HRESIMS spectrum of carbamidocyclophane F (2)
- Figure 9S. ^1H -NMR spectrum of carbamidocyclophane V (3)
- Figure 10S. ^{13}C -NMR spectrum of carbamidocyclophane V (3)
- Figure 11S. ^1H - ^1H COSY spectrum of carbamidocyclophane V (3)
- Figure 12S. HSQC spectrum of carbamidocyclophane V (3)
- Figure 13S. HMBC spectrum of carbamidocyclophane V (3)
- Figure 14S. NOESY spectrum of carbamidocyclophane V (3)
- Figure 15S. HRESIMS spectrum of carbamidocyclophane V (3)
- Figure 16S. ^1H -NMR spectrum of carbamidocylindrofridin A (4)
- Figure 17S. ^{13}C -NMR spectrum of carbamidocylindrofridin A (4)
- Figure 18S. ^1H - ^1H COSY spectrum of carbamidocylindrofridin A (4)
- Figure 19S. HSQC spectrum of carbamidocylindrofridin A (4)
- Figure 20S. HMBC spectrum of carbamidocylindrofridin A (4)
- Figure 21S. ECD of carbamidocylindrofridin A (4)
- Figure 22S. HRESIMS spectrum of carbamidocylindrofridin A (4)
- Table 1S. Sample and crystal data of carbamidocyclophane A (1)
- Table 2S. Data collection and structure refinement of carbamidocyclophane A (1)
- Table 3S. Relevant hydrogen bond parameters of carbamidocyclophane A (1)



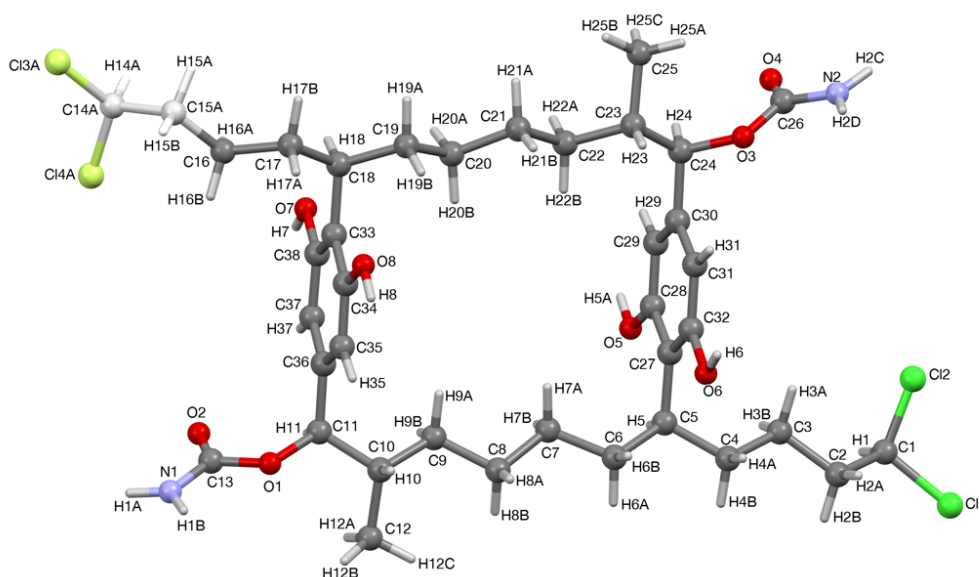
- Figure 1S. ¹H-NMR (500 MHz, CD₃OD) spectrum of carbamidocyclophane A (1)



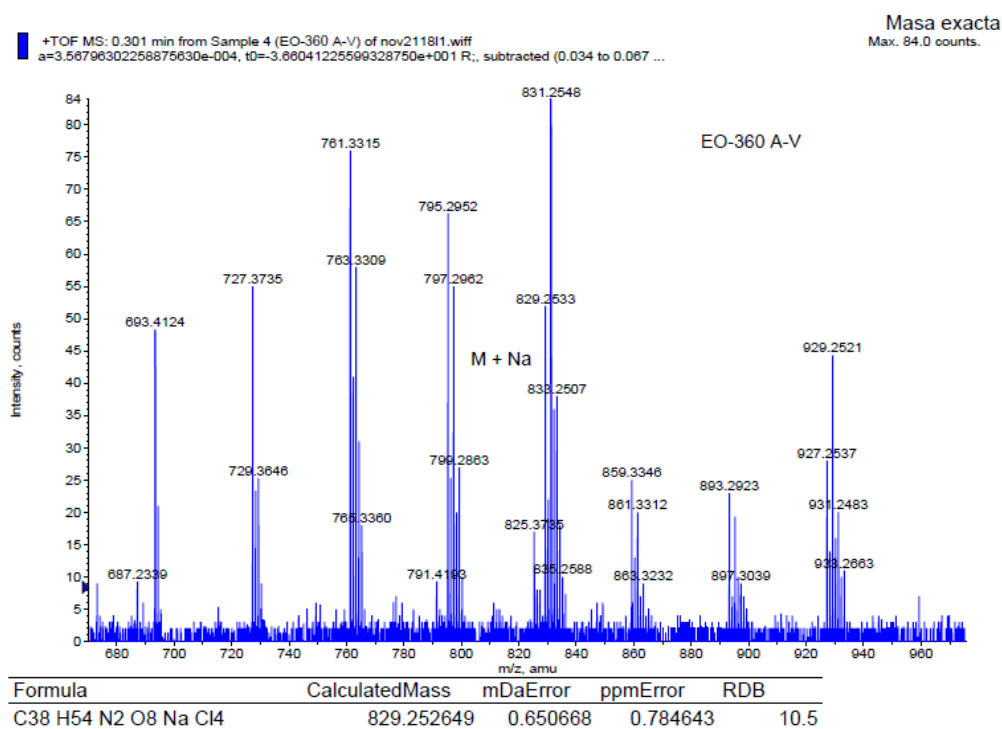
- Figure 2S. ¹³C-NMR (125 MHz, CD₃OD) spectrum of carbamidocyclophane A (1)



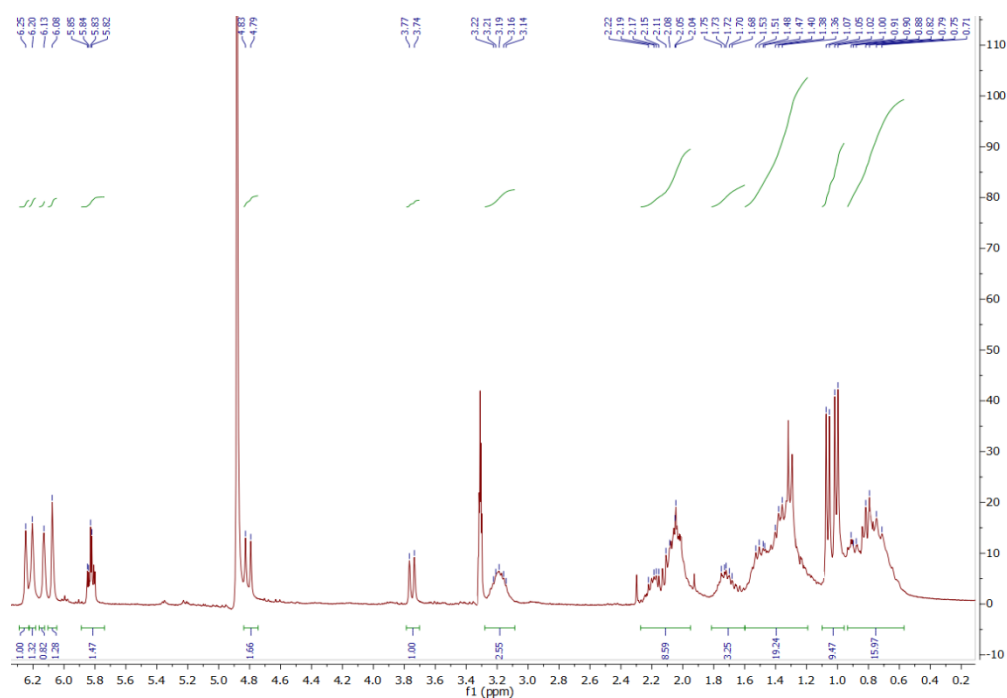
- Figure 3S. Hydrogen bonds found in carbamidocyclophane A (1); Hydrogen atoms not involved in these interactions have been omitted for clarity



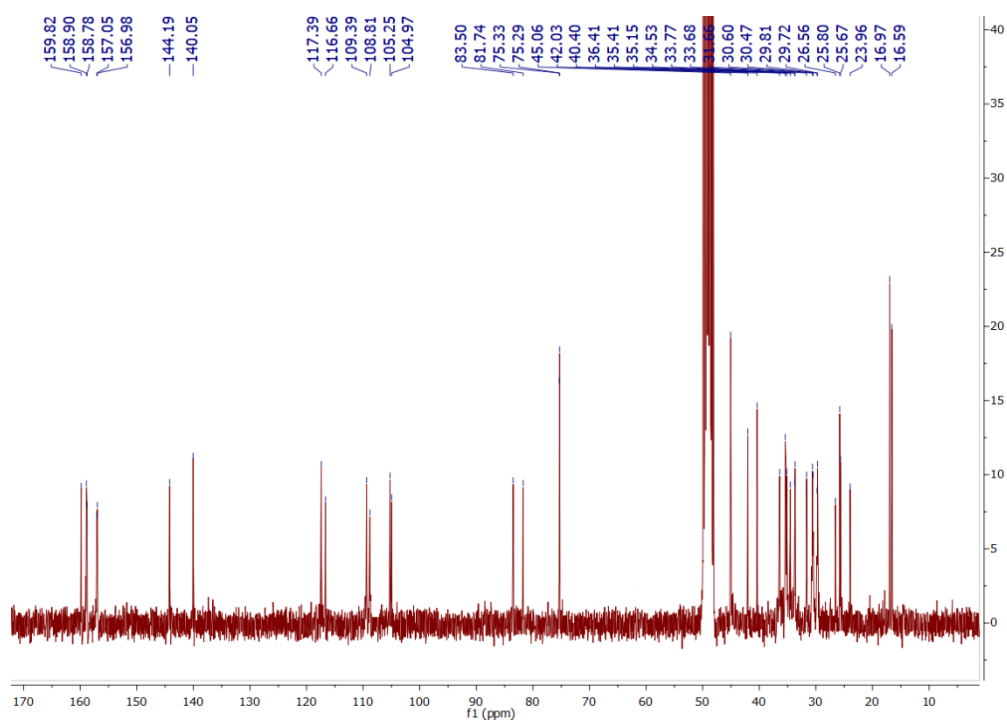
- Figure 4S. Labelled molecule of carbamidocyclophane A (1); carbon atoms C14A and C15A, hydrogen atoms H14A, H15A and H15B, and Cl3A, Cl4A (depicted in a lighter shade) only account for 50% of the expected electron density due to the disorder displayed by this part of the chain.



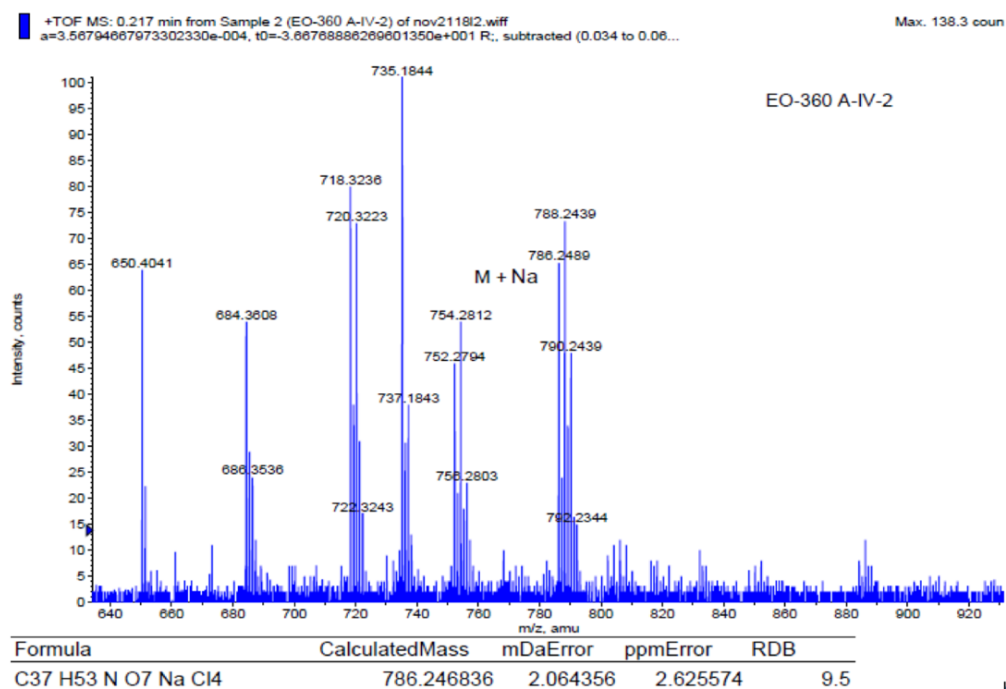
- Figure 5S. HRESIMS spectrum of carbamidocyclophane A (1)



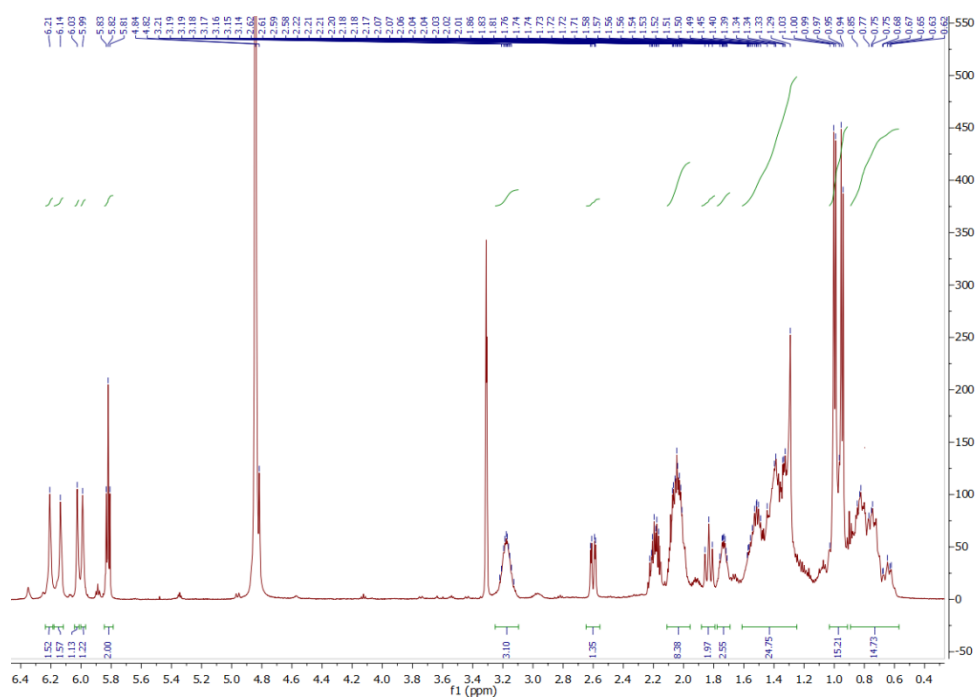
- Figure 6S. ¹H-NMR (500 MHz, CD₃OD) spectrum of carbamidocyclophane F (2)



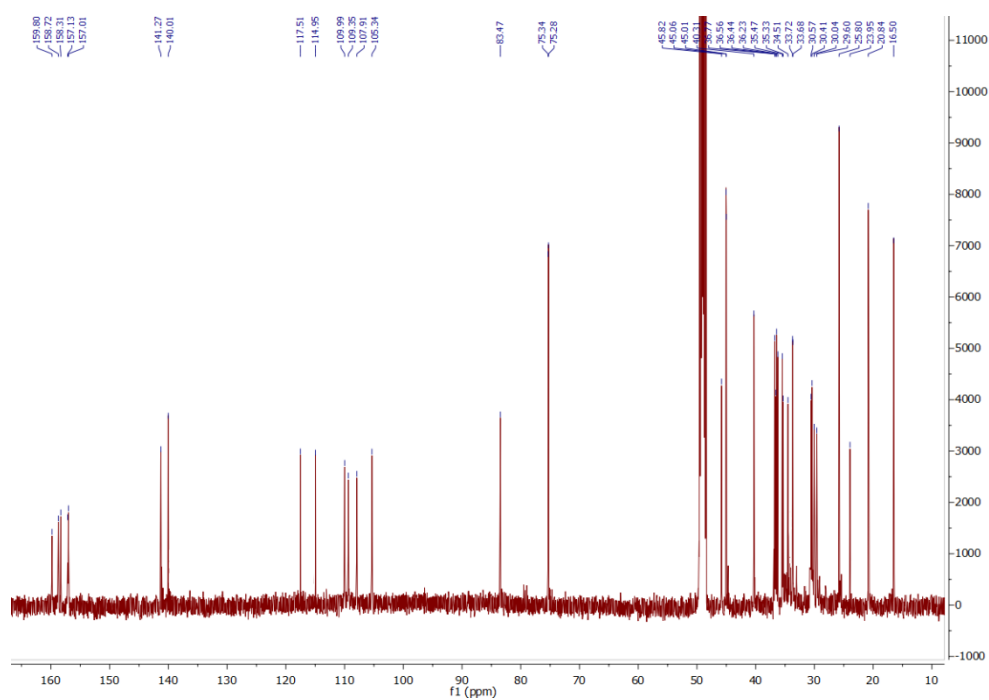
- Figure 7S. ^{13}C -NMR (125 MHz, CD_3OD) spectrum of carbamidocyclophane F (2)



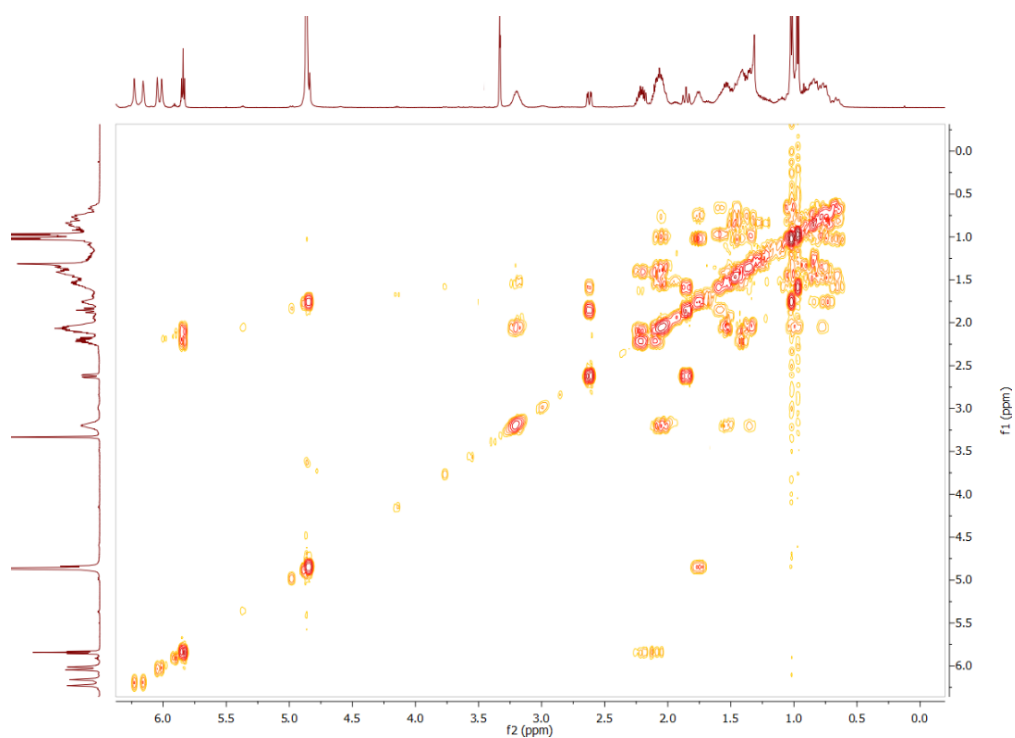
- Figure 8S. HRESIMS spectrum of carbamidocyclophane F (2)



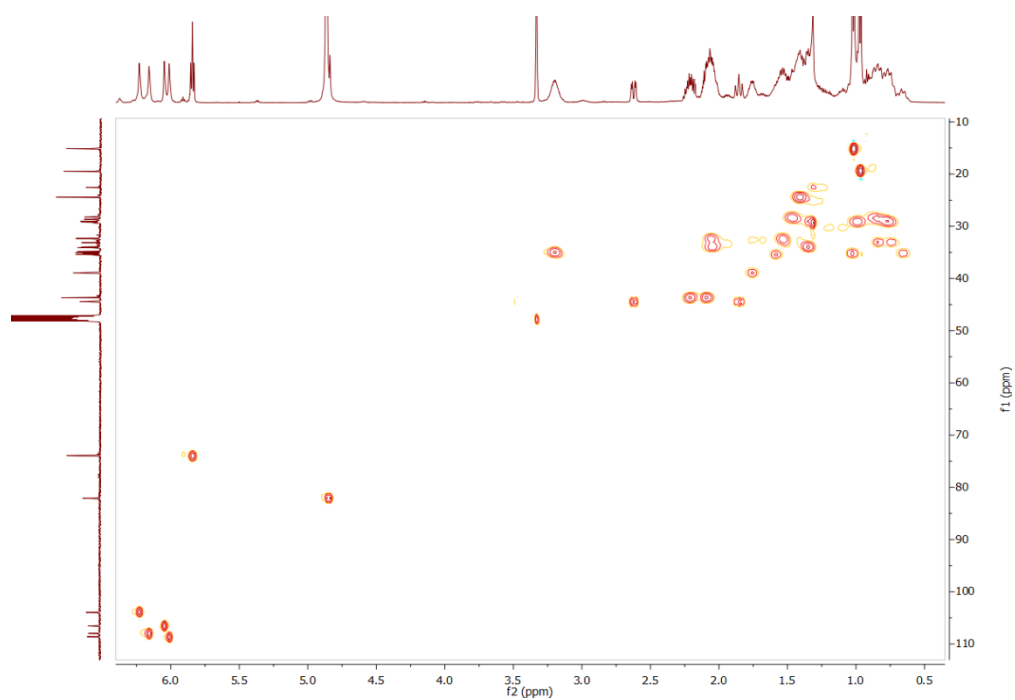
- Figure 9S. ^1H -NMR (500 MHz, CD_3OD) spectrum of carbamidocyclophane V (3)



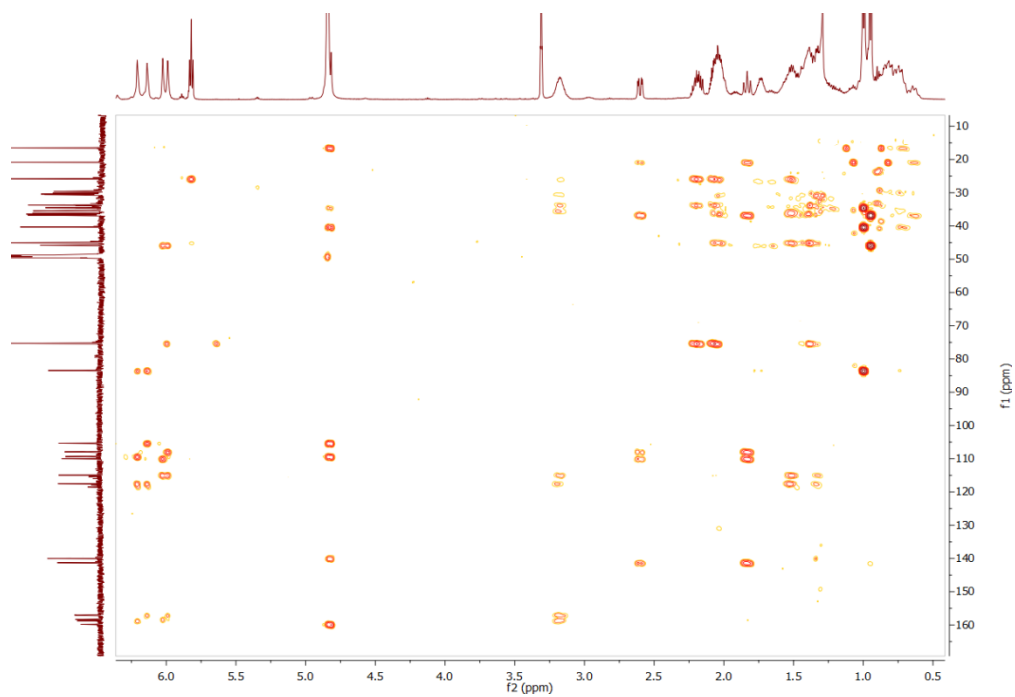
- Figure 10S. ^{13}C -NMR (125 MHz, CD_3OD) spectrum of carbamidocyclophane V (3)



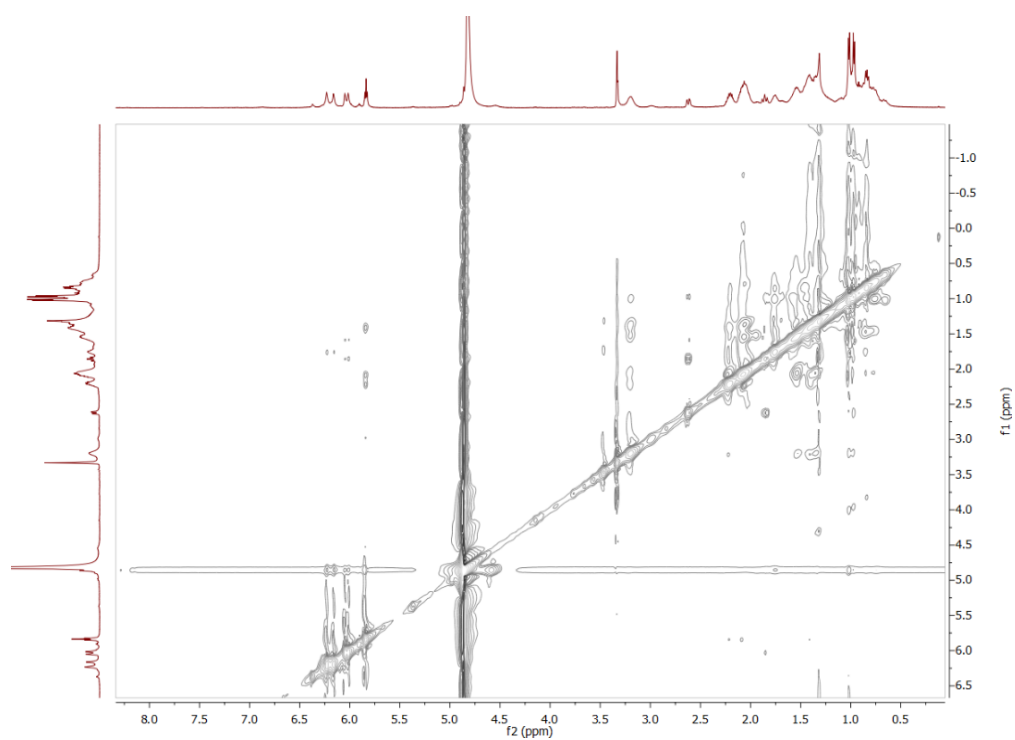
- Figure 11S. ^1H - ^1H COSY (CD_3OD) spectrum of carbamidocyclophane V (3)



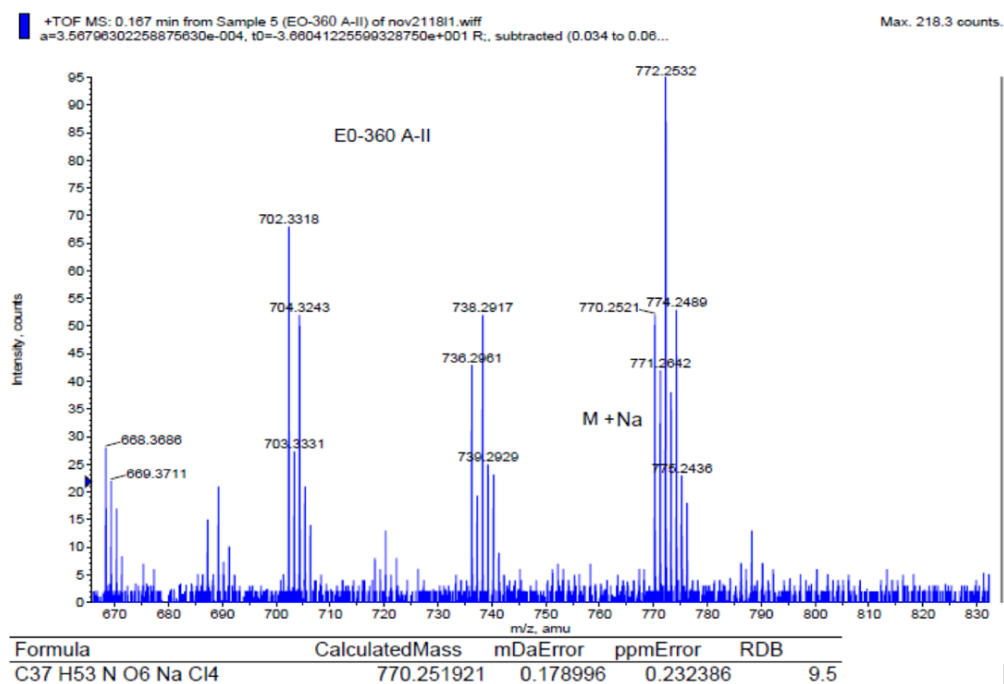
- Figure 12S. HSQC (CD_3OD) spectrum of carbamidocyclophane V (3)



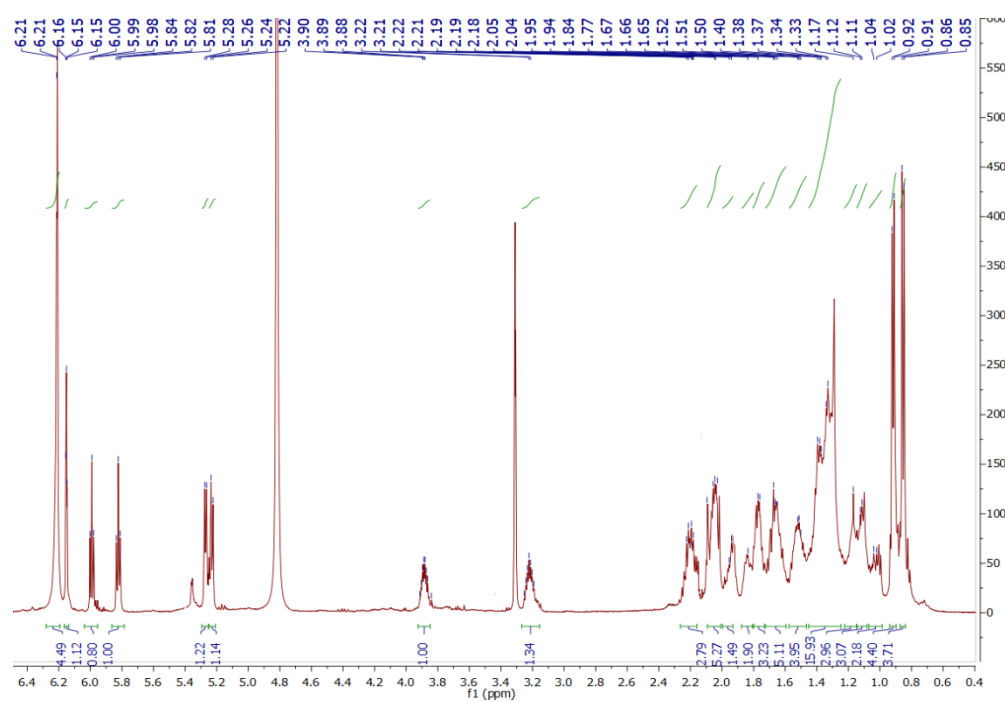
- Figure 13S. HMBC (CD₃OD) spectrum of carbamidocyclophane V (3)



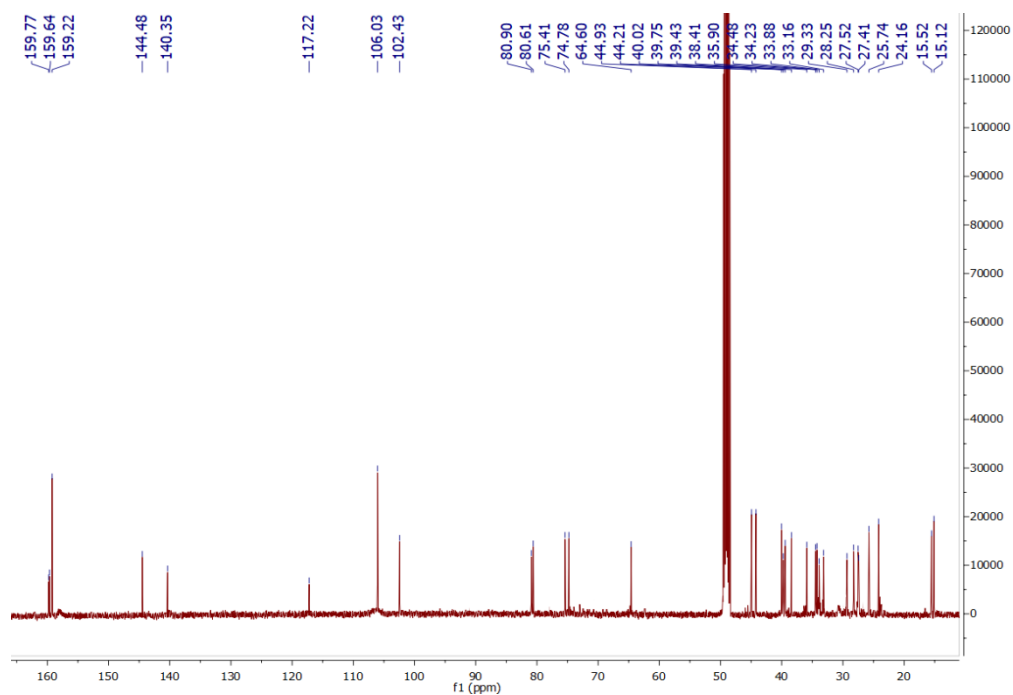
- Figure 14S. NOESY (CD₃OD) spectrum of carbamidocyclophane V (3)



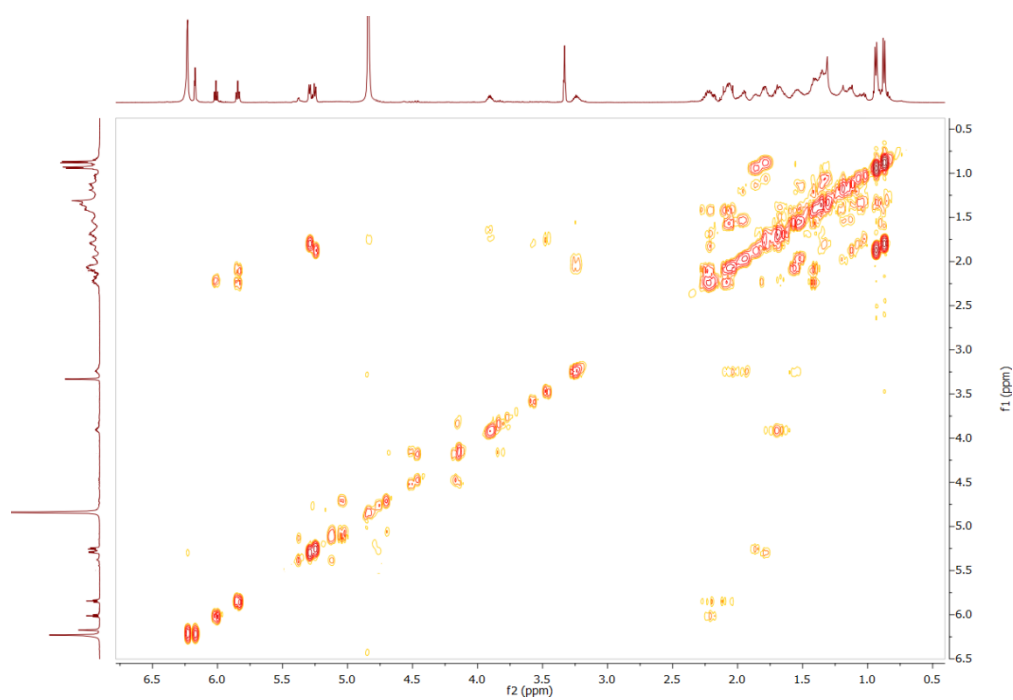
- Figure 15S. HRESIMS spectrum of carbamidocyclophane V (3)



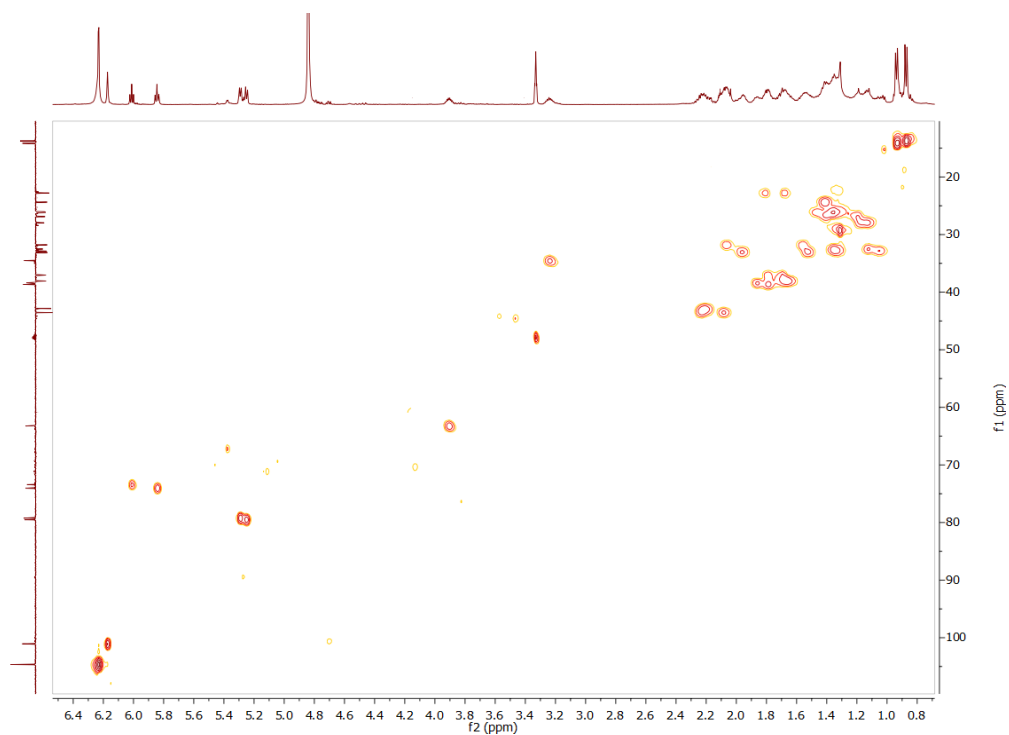
- Figure 16S. ¹H-NMR (500 MHz, CD₃OD) spectrum of carbamidocyclindrofridin A (4)



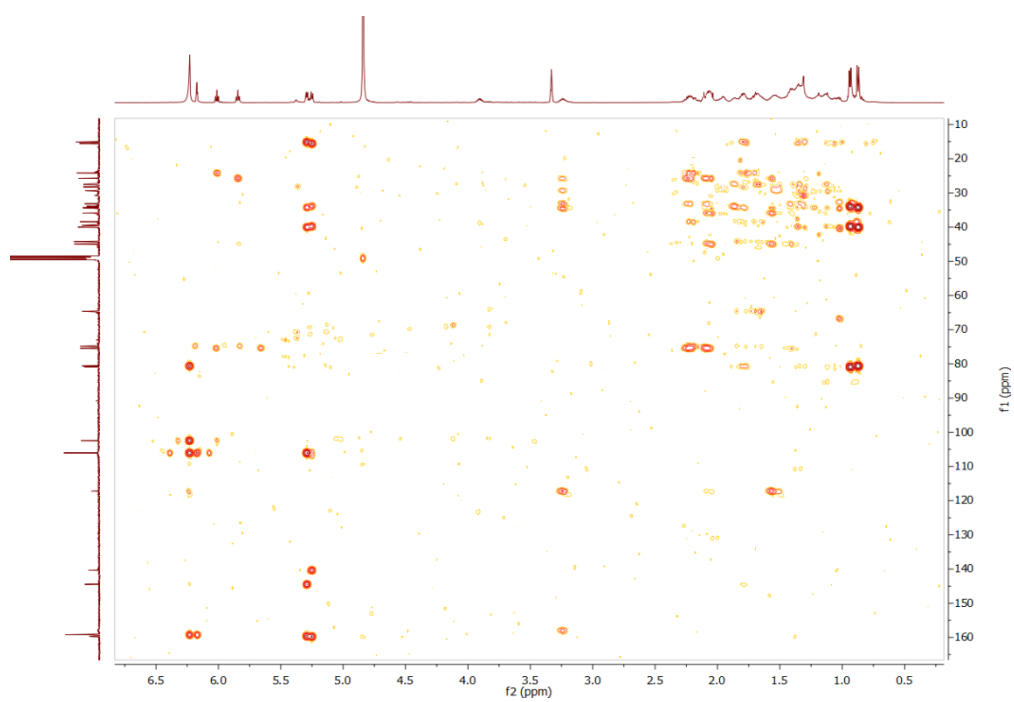
- Figure 17S. ^{13}C -NMR (125 MHz, CD_3OD) spectrum of carbamidocylindrofridin A (4)



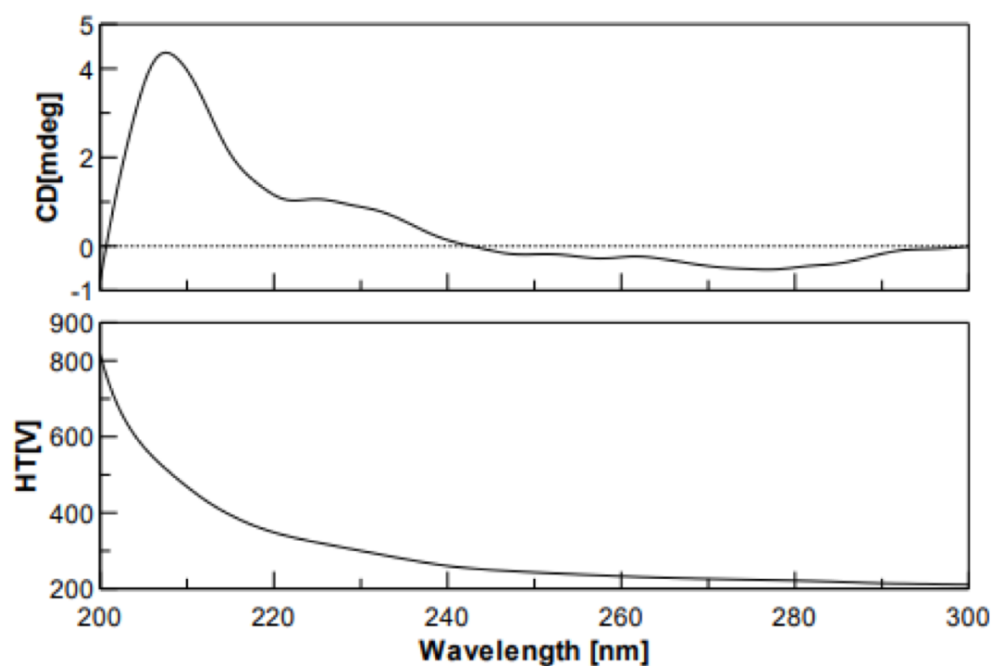
- Figure 18S. ^1H - ^1H COSY (CD_3OD) spectrum of carbamidocylindrofridin A (4)



- Figure 19S. HSQC (CD₃OD) spectrum of carbamidocylindrofridin A (4)



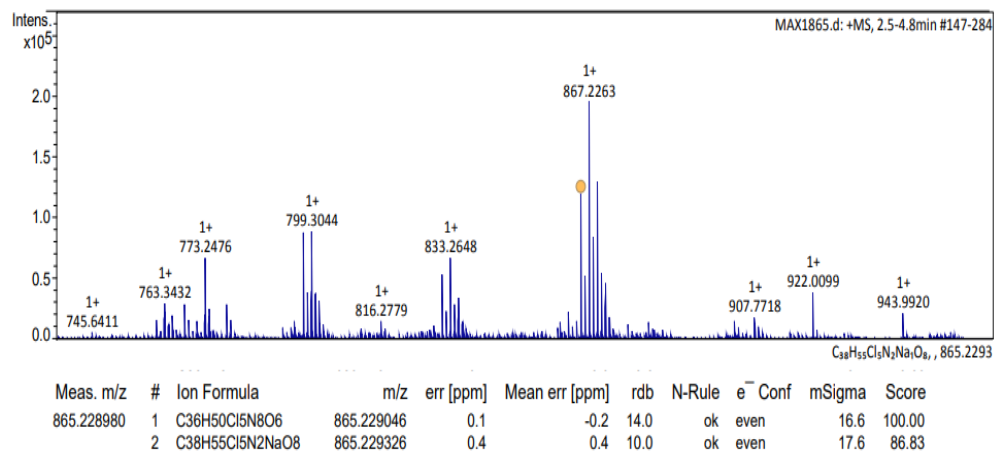
- Figure 20S. HMBC (CD₃OD) spectrum of carbamidocylindrofridin A (4)



- Figure 21S. ECD (CD₃OD) of carbamidocylindrofridin A (4)

Equipo MAXIS II

Nombre muestra EO-360-A-VI-2
 Nombre registro D:\Data\2019\2019_03 MARZO\MAX1865.d
 Metodo ESI Positive TOF_MS-50-3000.m
 Comentarios mg/ml en metanol. Dil 1:100 en metanol



- Figure 22S. HRESIMS spectrum of carbamidocylindrofridin A (4)

- Table 1S. Sample and crystal data of carbamidocyclophane A (1)

CCDC code	1969832	
Chemical formula	C ₅₂ H ₈₂ Cl ₄ N ₂ O ₁₄	
Formula weight	1101.02 g/mol	
Temperature	200(2) K	
Wavelength	0.71073 Å	
Crystal size	0.107 x 0.218 x 0.493 mm	
Crystal habit	clear colourless plate	
Crystal system	Monoclinic	
Space group	<i>P</i> 2 ₁	
Unit cell dimensions	<i>a</i> = 9.0920(6) Å	$\alpha = 90^\circ$
	<i>b</i> = 35.250(2) Å	$\beta = 115.077(2)^\circ$
	<i>c</i> = 10.1315(6) Å	$\gamma = 90^\circ$
Volume	2941.0(3) Å ³	
Z	2	
Density (calculated)	1.198 g/cm ³	
Absorption coefficient	0.227 mm ⁻¹	
F(000)	1136	

- Table 2S. Data collection and structure refinement of carbamidocyclophane A (1)

Theta range for data collection	1.16 to 25.35°
Index ranges	-10 ≤ <i>h</i> ≤ 10, -42 ≤ <i>k</i> ≤ 42, -12 ≤ <i>l</i> ≤ 12
Reflections collected	90850
Independent reflections	10751 [R(int) = 0.0527]
Coverage of independent reflections	100.0%
Absorption correction	multi-scan
Max. and min. transmission	0.9760 and 0.8960
Structure solution technique	direct methods
Structure solution program	SHELXS-97 (Sheldrick 2008)
Refinement method	Full-matrix least-squares on F ²
Refinement program	SHELXL-2014/7 (Sheldrick, 2014)
Function minimized	$\Sigma w(F_o^2 - F_c^2)^2$
Data / restraints / parameters	10751 / 7 / 663

Goodness-of-fit on F²	1.053	
Final R indices	8588 data; I>2σ(I)	R1 = 0.0955, wR2 = 0.2603
	all data	R1 = 0.1151, wR2 = 0.2845
Weighting scheme	w=1/[σ ² (F _o ²)+(0.1909P) ² +2.3614P]where P=(F _o ² +2F _c ²)/3	
Absolute structure parameter	0.1(0)	
Largest diff. peak and hole	1.144 and -0.613 eÅ ⁻³	

- Table 3S. Relevant hydrogen bond parameters of carbamidocyclophane A (1)

	Donor-H	Acceptor...H	Donor...Acceptor	Angle
N1-H1A...O4ⁱ	0.88	2.08	2.945(9)	167.5
N2ⁱ-H2C...O2	0.88	1.98	2.850(8)	172.5
O5-H5...O10ⁱⁱ	0.84	2.01	2.82(1)	161.8
O6-H6...O13	0.84	1.94	2.71(1)	152.0
O7-H7...O11	0.84	2.00	2.76(1)	149.2
O8-H8...O9ⁱⁱⁱ	0.84	2.21	2.99(1)	153.9
Symmetry operations i= 1-x, -1/2+ y, 1-z; ii= 1+x, y, 1+z; iii=-1+x, y, z				